

BRIEF COMMUNICATIONS

Luminescence of the Te^{4+} Ion in ZrP_2O_7

H. DONKER, M. J. DEN EXTER, W. M. A. SMIT, AND G. BLASSE

*Physics Laboratory, University of Utrecht, P.O. Box 80000,
3508 TA Utrecht, The Netherlands*

Received February 13, 1989

The luminescence spectra and decay times of the Te^{4+} ion in ZrP_2O_7 are reported and discussed. $\text{ZrP}_2\text{O}_7:\text{Te}^{4+}$ shows a blue emission band with a maximum at $21,200\text{ cm}^{-1}$ at LHeT. Decay time measurements reveal the presence of at least two kinds of Te^{4+} ions. This is not apparent from the luminescence spectra, indicating that the Te^{4+} ions have quite similar environments. The $^1S_0 \rightarrow ^3P_1$ excitation band of the Te^{4+} ion is situated at $38,250\text{ cm}^{-1}$. A comparison is made with the luminescence of related systems. © 1989 Academic Press, Inc.

1. Introduction

Recently a number of papers have been published on the luminescence of Te^{4+} in antifluorite type halides (1–8). Very little is known about the luminescence of Te^{4+} in other systems. Therefore, we investigated the luminescence of Te^{4+} in an oxidic host lattice, viz., ZrP_2O_7 . Zirconium pyrophosphate has a cubic crystal structure which offers an octahedral site to the tetravalent metal ions (9), and is therefore expected to be an interesting host lattice to study the luminescence of Te^{4+} . A comparison is made with the luminescence of $\text{Cs}_2\text{ZrCl}_6:\text{Te}^{4+}$, $\text{Cs}_2\text{NaScCl}_6:\text{Sb}^{3+}$, and $\text{Sc}(\text{PO}_3)_3:\text{Sb}^{3+}$.

2. Experimental

Starting materials were $\text{ZrOCl}_2 \cdot 8\text{H}_2\text{O}$ (Merck, p.a.), $(\text{NH}_4)_2\text{HPO}_4$ (Merck, p.a.), and TeO_2 (Merck, 99.999%). Samples were

prepared by firing stoichiometric quantities of $\text{ZrOCl}_2 \cdot 8\text{H}_2\text{O}$, TeO_2 , and $(\text{NH}_4)_2\text{HPO}_4$ at 1000°C for 4 hr in air. The weighed-in concentration of Te^{4+} was 1 mol%. Samples were checked by X-ray powder diffraction using $\text{CuK}\alpha$ radiation.

Diffuse reflectance spectra were measured at room temperature (RT) on a Perkin-Elmer Lambda 7 UV/VIS spectrophotometer. Emission spectra were recorded on a Perkin-Elmer MPF 44B spectrofluorometer equipped with an Oxford CF204 liquid helium flow cryostat. The emission spectra were corrected for photomultiplier sensitivity. The photon flux per constant energy interval (Φ) is obtained by multiplying the radiant power per constant wavelength interval by λ^3 . The instrumental setup for the measurement of the excitation spectra has been described before (10).

Decay curves were recorded with a single photon counting system. The excitation source consists of an Edinburgh Instru-

ments 199F coaxial flashlamp filled with deuterium. Excitation and emission wavelengths were selected by means of bandpass filters. For detection an RCA C31034 photomultiplier tube was used in combination with an Ortec 574 fast timing amplifier, an Ortec 436 100-MHz discriminator, an Ortec 467 time to pulse height converter, and a Nucleus Personal Computer Analyzer 4000 card which was built in an Olivetti M24 Personal Computer. In this setup the sample was immersed in liquid helium in a Thor cryogenics S-100 bath cryostat. The temperature of the sample could be regulated between 1.7 and 300 K using a Thor cryogenics Model 3020 temperature controller. The temperature was measured using a carbon glass resistance thermometer.

3. Results

The diffuse reflectance spectrum of undoped ZrP_2O_7 shows that the host lattice absorption starts at about $43,500\text{ cm}^{-1}$. The diffuse reflectance spectrum of $\text{ZrP}_2\text{O}_7:\text{Te}^{4+}$ shows an additional absorption band at about $38,000\text{ cm}^{-1}$. Upon excitation into this band a blue emission is observed. The emission spectrum at liquid helium temperature (LHeT) is shown in Fig. 1. The maximum of the emission band is situated at $21,200\text{ cm}^{-1}$. The emission intensity starts to quench at about 70 K, and at RT only 4% of the original intensity is left.

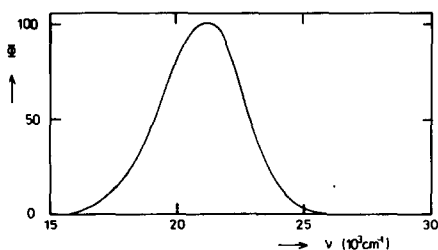


FIG. 1. Emission spectrum of $\text{ZrP}_2\text{O}_7:\text{Te}^{4+}$ (1 mol%) at LHeT. Φ denotes the photon flux per constant energy interval in arbitrary units.

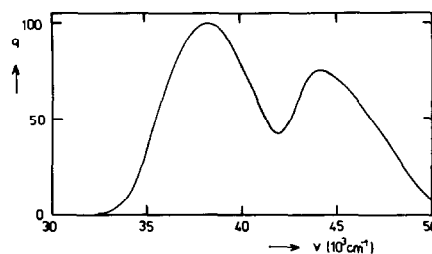


FIG. 2. Excitation spectrum of the Te^{4+} emission of $\text{ZrP}_2\text{O}_7:\text{Te}^{4+}$ (1 mol%) at LHeT. q denotes the relative quantum output in arbitrary units.

The excitation spectrum of the blue emission band is shown in Fig. 2. There are two excitation bands. One with a maximum at about $38,250\text{ cm}^{-1}$ in agreement with the diffuse reflectance spectrum and a somewhat weaker band at about $44,150\text{ cm}^{-1}$. At RT these bands shift to $37,500$ and $43,700\text{ cm}^{-1}$, respectively. The intensity ratio between these bands remains approximately constant.

Decay time measurements were performed as a function of temperature. The samples were excited in the $38,250\text{-cm}^{-1}$ excitation band. All measured decay curves could be satisfactorily fitted to a biexponential decay function. The temperature dependence of both decay times shows a drastic change in the 4–30 K region (see Fig. 3). Since the intensity of the emission band remains constant in this temperature region, the experimental data were fitted to a three-level scheme (11). The temperature dependence of the decay time can then be expressed as

$$1/\tau = \frac{(1/\tau_1) + (1/\tau_2) \exp(-\Delta E/kT)}{1 + \exp(-\Delta E/kT)}. \quad (1)$$

In this equation τ_1 and τ_2 denote the radiative decay times of the 3P_0 and 3P_1 levels, respectively. The energy difference between these levels in the relaxed excited state is denoted by ΔE . The degeneracies of the levels involved has been neglected. The drawn lines in Fig. 3 represent the best fits

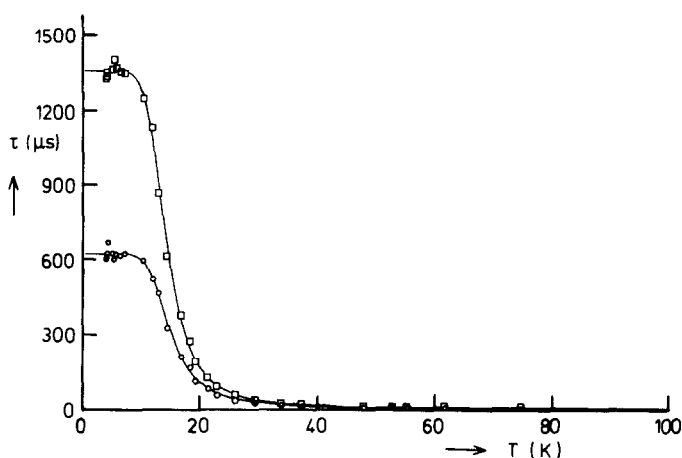


FIG. 3. Temperature dependence of the two decay times of the Te^{4+} emission of $\text{ZrP}_2\text{O}_7:\text{Te}^{4+}$ (1 mol%). The drawn lines are the best fits to Eq. (1).

of the experimental data to Eq. (1). The resulting parameters are $\tau_1 = (621 \pm 4) \mu\text{sec}$, $\tau_2 = (1.1 \pm 0.2) \mu\text{sec}$, $\Delta E = (66 \pm 2) \text{cm}^{-1}$ for the faster component, and $\tau_1 = (1360 \pm 7) \mu\text{sec}$, $\tau_2 = (1.6 \pm 0.3) \mu\text{sec}$, $\Delta E = (67 \pm 2) \text{cm}^{-1}$ for the slower component. The intensity ratio between the faster and the slower component is about 1.6.

4. Discussion

The emission band at $21,300 \text{cm}^{-1}$ is ascribed to the ${}^3P_0, {}^3P_1 \rightarrow {}^1S_0$ transitions on the Te^{4+} ion. At low temperatures the emission originates mainly from the 3P_0 level, while at higher temperatures the 3P_1 level is also occupied. This is confirmed by the temperature dependence of the decay times. The long decay times at low temperatures reflect the forbidden character of the ${}^3P_0 \rightarrow {}^1S_0$ transition.

The decay time measurements reveal further that the $21,200\text{-cm}^{-1}$ emission band consists of at least two components. This cannot be ascribed to the presence of $(\text{Te}^{4+})_2$ centers since paired s^2 ions usually have emission and excitation bands at considerably lower energy than those of isolated s^2 ions (12, 13). It has been shown that

ZrP_2O_7 exists in several modifications, in which the geometry of the $\text{P}_2\text{O}_7^{4-}$ groups is slightly different (14–16). Our samples consist of what is called the ZrP_2O_7 (II) modification. For SiP_2O_7 (II), which is probably isostructural with ZrP_2O_7 (II), a computer simulation revealed the presence of six slightly different Si sites (17). Therefore, the experimentally observed decay curves are most probably due to Te^{4+} ions on slightly different sites in the ZrP_2O_7 host lattice.

The excitation band at $38,250 \text{cm}^{-1}$ is ascribed to the ${}^1S_0 \rightarrow {}^3P_1$ transition on the Te^{4+} ion (A-band). The nature of the $44,150\text{-cm}^{-1}$ excitation band is not entirely clear. It cannot be ascribed to the ${}^1S_0 \rightarrow {}^3P_2$ transition, which is expected to gain intensity upon increasing the temperature. A better possibility is to ascribe this band to the ${}^1S_0 \rightarrow {}^1P_1$ transition, although this requires that the $44,150\text{-cm}^{-1}$ band be much stronger than the ${}^1S_0 \rightarrow {}^3P_1$ excitation band. However, the competitive host lattice absorption which starts at about $43,500 \text{cm}^{-1}$ could explain the low intensity of the ${}^1S_0 \rightarrow {}^1P_1$ excitation band. There is, however, another explanation possible for the $44,150\text{-cm}^{-1}$ excitation band. The zirconate emis-

TABLE I
COMPARISON OF SPECTRAL DATA OF $ZrP_2O_7:Te^{4+}$
WITH RELATED SYSTEMS

Composition	A-band	Emission band	Stokes shift	ΔE	Ref.
$ZrP_2O_7:Te^{4+}$	38,250	21,200	17,050	66.67	This work
$Cs_2ZrCl_6:Te^{4+}$	25,100	17,200	7,400	109	(7)
$Sc(PO_3)_3:Sb^{3+}$	40,000	24,700	15,300	39.45	(28)
$Cs_2NaScCl_6:Sb^{3+}$	31,000	22,700	7,500	110	(21)

Note. All data are in cm^{-1} .

sion of ZrP_2O_7 is situated at about $35,000\text{ cm}^{-1}$ (18) and has a good spectral overlap with the $^1S_0 \rightarrow ^3P_1$ excitation band of the Te^{4+} ions. Therefore, it is also possible that the $44,150\text{-cm}^{-1}$ excitation band is due to energy transfer from the zirconate groups to the Te^{4+} ions.

The present data on the Te^{4+} emission in an oxidic host lattice agree reasonably well with those reported before for the tellurite antiglass phases where the tellurium concentration is much higher (19, 20). In Table I the spectral data for $ZrP_2O_7:Te^{4+}$ are compared with similar data for $Cs_2ZrCl_6:Te^{4+}$, $Cs_2NaScCl_6:Sb^{3+}$, and $Sc(PO_3)_3:Sb^{3+}$. The $^1S_0 \rightarrow ^3P_1$ excitation band of $ZrP_2O_7:Te^{4+}$ is at much higher energy than that in $Cs_2ZrCl_6:Te^{4+}$, which is due to the fact that the pyrophosphate group is less covalent toward the Te^{4+} ion than the chloride ion. Just as for Sb^{3+} , the Stokes shift for the Te^{4+} luminescence in the phosphate is larger than that in the chloride, and the value of ΔE is smaller. For s^2 ions it is generally found that ΔE decreases for increasing values of the Stokes shift (21–24). This has been explained in terms of quenching of the spin–orbit interaction by the Jahn–Teller effect (25). However, the decrease of ΔE with the Stokes shift in the phosphates is rather small. This suggests that the larger Stokes shifts in the phosphates are not entirely due to a stronger Jahn–Teller effect. There are two alternative explanations which are probably both of influence.

(a) In two earlier papers (7, 26) we reported that the Stokes shift increases for a decreasing degree of covalency due to a contribution of a shift along the totally symmetric vibrational coordinate. Since the phosphates are less covalent than the chlorides, larger Stokes shifts are expected.

(b) In a simple configurational coordinate diagram the Stokes shift is given by $\Delta E_s = (2S - 1)\hbar\omega$ (27), where S is the Huang–Rhys coupling and ω the vibrational frequency involved. The latter will be higher in oxides than in chlorides, so that for the same coupling strength the Stokes shift ΔE_s is expected to be larger in an oxide than in a chloride.

Finally, we note that as a consequence of the presence of slightly different Te^{4+} ions and the large Stokes shift of the emission of $ZrP_2O_7:Te^{4+}$ we have lost all vibrational structure in the Te^{4+} emission band. In $Cs_2ZrCl_6:Te^{4+}$ this structure was very pronounced (6, 7).

In conclusion we have reported the first case of an emitting Te^{4+} activator in an oxidic host lattice.

References

1. R. WERNICKE, H. KUPKA, W. ENSSLIN, AND H.-H. SCHMIDTKE, *Chem. Phys.* **47**, 235 (1980).
2. G. BLASSE, G. J. DIRKSEN, AND P. A. M. BERDOWSKI, *Chem. Phys. Lett.* **112**, 313 (1984).
3. G. BLASSE, G. J. DIRKSEN, AND W. ABRIEL, *Chem. Phys. Lett.* **136**, 460 (1987).
4. J. F. ACKERMAN, *Mat. Res. Bull.* **19**, 783 (1984).
5. K. MEIDENBAUER AND G. GLIEMANN, *Z. Naturforsch.* **A39**, 555 (1988).
6. P. J. H. DRUMMEN, H. DONKER, W. M. A. SMIT, AND G. BLASSE, *Chem. Phys. Lett.* **144**, 460 (1988).
7. H. DONKER, W. M. A. SMIT, AND G. BLASSE, *J. Phys. Chem. Solids* **50**, 603 (1989).
8. J. DEGEN AND H.-H. SCHMIDTKE, *Chem. Phys.* **129**, 483 (1989).
9. R. W. G. WYKOFF, "Crystal Structures," Vol. II, p. 428, Wiley, New York (1963).
10. E. W. J. L. OOMEN, W. M. A. SMIT, AND G. BLASSE, *Phys. Rev. B* **37**, 18 (1988).
11. G. BOULON, C. PÉDRINI, M. GUIDONI, AND CH. PANNEL, *J. Phys.* **36**, 267 (1975).

12. A. ERMOSHKIN, R. EVARESTOV, R. GINDINA, A. MAAROOS, V. OSMININAND, AND S. ZAZOBOVICH, *Phys. Stat. Sol. (b)* **70**, 749 (1975).
13. N. YAMASHITA AND S. ASANO, *J. Phys. Soc. Japan* **41**, 536 (1976).
14. M. CHAUNAC, *Bull. Soc. Chim.*, 424 (1971).
15. R. PASCARD, M. CHAUNAC, AND E. GRISON, *Bull. Soc. Chim.*, 429 (1971).
16. C.-H. HUANG, O. KNOP, D. A. OTHEN, F. W. D. WOODHAMS, AND R. A. HOWIE, *Canad. J. Chem.* **53**, 79 (1975).
17. E. TILLMANS, W. GIBERT, AND W. H. BAUR, *J. Solid State Chem.* **7**, 69 (1973).
18. A. BRIL AND H. A. KLASENS, *Philips Res. Rep.* **7**, 421 (1952).
19. G. BLASSE, G. J. DIRKSEN, E. W. J. L. OOMEN, AND M. TRÖMEL, *J. Solid State Chem.* **63**, 148 (1986).
20. M. TRÖMMEL, E. MÜNCH, G. BLASSE, AND G. J. DIRKSEN, *J. Solid State Chem.* **76**, 345 (1988).
21. G. BLASSE AND A. C. VAN DER STEEN, *Solid State Commun.* **31**, 993 (1979).
22. E. W. J. L. OOMEN, W. M. A. SMIT, AND G. BLASSE, *J. Phys. C* **19**, 3263 (1986).
23. E. W. J. L. OOMEN, W. M. A. SMIT, AND G. BLASSE, *J. Phys. C* **20**, 1161 (1987).
24. E. W. J. L. OOMEN, L. C. G. VAN GORKOM, W. M. A. SMIT, AND G. BLASSE, *J. Solid State Chem.* **65**, 156 (1986).
25. D. MUGNAI, A. RANFAGNI, O. PILLA, G. VILIANI, AND M. MONTAGNA, *Solid State Commun.* **35**, 975 (1980).
26. H. DONKER, W. M. A. SMIT, AND G. BLASSE, *Phys. Stat. Sol. (b)* **145**, 333 (1988).
27. G. F. IMBUSH, in "Luminescence Spectroscopy" (M. D. Lumb, Ed.), Chap. 1, Academic Press, London (1978).
28. E. W. J. L. OOMEN, R. C. M. PEETERS, W. M. A. SMIT, AND G. BLASSE, *J. Solid State Chem.* **73**, 151 (1988).